

Characterization and fine mapping of *nonstop glumes 2 (nsg2)* mutant in rice (*Oryza sativa* L.)

Yunfeng Li^{*,†}, Xiaoqin Zeng[†], Hui Zhuang, Huan Chen, Ting Zhang, Jun Zhang, Hao Zheng, Jun Tang, Honglei Wang, Suxian Ren, Yinghua Ling, Guanghua He^{**}

Rice Research Institute, Key Laboratory of Application and Safety Control of Genetically Modified Crops, Academy of Agricultural Sciences, Southwest University, Chongqing 400715, China

*E-mail: liyf1980@swu.edu.cn Tel: +86-023-68250158 Fax: +81-023-68250158

**E-mail: heghswu@163.com Tel: +86-023-68250158 Fax: +81-023-68250158

Received November 28, 2018; accepted May 6, 2019 (Edited by H. Shimada)

Abstract In cereal crops, the grain number per panicle and the grain yield are greatly affected by the number of florets in a spikelet. In wild-type rice, a spikelet only produces one fertile floret and beneath the floret are a pair of sterile lemmas and a pair of rudimentary glumes. This study characterized a rice spikelet mutant *nonstop glumes 2 (nsg2)*. In the *nsg2* mutant, both the sterile lemmas and rudimentary glumes were elongated, and part of sterile lemma looked like a lemma in appearance, shape and size. Detailed histological analysis and qPCR analysis revealed that the sterile lemmas in the *nsg2* mutant had homeotically transformed into lemma-like organs. This phenotype indicates that *NSG2* is involved in the regulation of spikelet development and supports the long-held view that sterile lemmas were derived from the lemmas of the two lateral florets. This implies that the rice spikelet has the potential to be restored to the “three florets spikelet”, which may have existed in its ancestors. Genetic analysis reveals that the *nsg2* trait is controlled by a single recessive gene. The *NSG2* gene was finally mapped between markers R-20 and R-39 on chromosome 7 with a physical region of 180 kb. The two MYB family factors *LOC_Os07g44030* and *LOC_Os07g44090* might be involved in the development of the spikelet and floral organ, and they were considered as candidate genes of *NSG2*. These results provide a foundation for map-based cloning and function analysis of *NSG2*, as well as evidence to support “three-florets spikelet” breeding in rice.

Key words: gene mapping, *nonstop glumes 2 (nsg2)*, rice (*Oryza sativa*), spikelet.

Introduction

The development process and the structure of the panicle and flower have important effects on yield and quality in crops. A major change in the life of a plant occurs during the transition from vegetative to reproductive growth. The shoot apical meristem (SAM) stops initiating leaves and transforms into the inflorescence meristems (IMs); later, the IMs transform into floral meristems (FMs), and FMs transform into floral organs. In rice, the IMs are not directly transformed into FMs, but are first transformed into spikelet meristems (SMs), and the SMs are then transformed into FMs to form florets (McSteen et al. 2000; Schmidt and Ambrose 1998). In rice, the panicle consists of primary branches, secondary branches, and spikelets on the branches. The grain number per panicle is correlated mainly with the primary and secondary branches. *OsCKX2/Gn1a*, *Ghd7*, *DENSE AND ERECT PANICLE 1 (DEP1)*, *DEP2* and *OsSPL14/IPA1* have been applied to increase yield by regulating panicle branching

in rice (Ashikari et al. 2005; Li et al. 2010; Miura et al. 2010; Xue et al. 2008; Yan et al. 2007). In rice and other *Oryzaeae*, the spikelet is the primary unit of inflorescence but only produce one fertile floret, while it can produce one or more florets in some other grasses, such as wheat. Therefore, increasing the number of florets in a spikelet may provide a new path to improve yield in those one-floret/grain spikelet species, such as rice. As a consequence, there is a need for a better understanding of the genetic and molecular mechanism of spikelet development.

In rice, each spikelet generates a single floret (also known as a terminal floret). A pair of sterile lemmas are formed outside of the floret, and a pair of rudimentary glumes are formed below the sterile lemma. The terminal floret consists of one lemma, one palea, two lodicules, six stamens and one carpel. It is generally thought that the rudimentary glumes are equivalent to the degraded glumes of other grasses. Regarding the origin and evolution of the sterile lemmas, there have

[†]These authors contributed equally to this work.
This article can be found at <http://www.jspcmb.jp/>
Published online September 21, 2019

been two prevailing hypotheses. The first holds that sterile lemmas and rudimentary glumes are both the result of degradation of the glume (Hong et al. 2010; Schmidt and Ambrose 1998; Terrell et al. 2001). The second hypothesis proposes that the spikelet of rice ancestors contained a top floret and two lateral florets. It is supposed that the rice spikelet was a “three-florets spikelet”, and the lateral florets degenerated into sterile lemmas during the evolution of the modern plant (Kellogg 2009; Kobayashi et al. 2010; Yoshida et al. 2009). Recently, several studies have supported this “three-florets spikelet” hypothesis. *LONG STERILE LEMMA* (*G1*), a plant-specific gene, encodes a DUF640 protein. In the *g1* mutant, the sterile lemma is larger than that of the wild-type, and has structural features resembling those of the lemma in the top fertile floret (Yoshida et al. 2009). The gene *EXTRA GLUME 1* (*EG1*) encodes a lipase. The *eg1* mutant develops lemma-like sterile lemmas, suggesting that *EG1* specifies the sterile lemma identity (Li et al. 2009). Another gene, *OsMADS34/PAP2*, also regulates the development of the sterile lemma. In the *osmads34* mutant, the sterile lemmas are transformed into the lemmas and have the lemma identity (Gao et al. 2010; Kobayashi et al. 2010, 2012). Mutations of *NONSTOP GLUME* (*NSG*) and *ABERRANT SPIKELET AND PANICLE1* (*ASPI1*) also lead to lemma-like sterile lemma (Kwon et al. 2012; Wang et al. 2013; Yoshida et al. 2012). Moreover, the *OsMADS1/LEAFY HULL STERILE 1* gene controls the development of the lemma and palea. Expression of *OsMADS1* is almost absent in the sterile lemma, but the ectopic expression of *OsMADS1* causes a homeotic transformation from a sterile lemma into a lemma (Agrawal et al. 2005; Prasad et al. 2001, 2005; Wang et al. 2017). These results suggested that sterile lemmas were the degraded lemma of two lateral florets in rice. Recently, a gain-of-function mutant *lateral florets 1* (*lf1*) in rice has been reported (Zhang et al. 2017). In *lf1*, the spikelet develops lateral florets with proper floral organ identities in the axil of the sterile lemma, providing direct evidence for the “three-florets” hypothesis.

In summary, all of the above studies suggest that the spikelet of the ancestor of rice may be a “three-florets” spikelet. And to become its present form, a group of genes are involved in the identity specification of the sterile lemma during the evolution. However, to better understand the gene regulation network of sterile lemma (lateral florets) development and evolution, more related mutants and researches on these mutants are needed in rice. In this study, a novel sterile lemma mutant *nonstop glumes 2* (*nsg2*) was reported. The sterile lemmas of *nsg2* mutant were elongated and were believed to have gained the lemma-like identity. In addition to phenotype analysis, we also performed gene mapping to locate the candidate gene in this study. This provided a foundation for map-based cloning of *NSG2* and its function analysis.

Materials and methods

Materials

We obtained the abnormal glume mutant *nsg2* by EMS mutagenesis of the indica maintainer line *Xinong 1B* (Supplementary Figure S1A). The *nsg2* mutant was then crossed with sterile line 56S (indica) (Supplementary Figure S1B) to yield the F₁ population (Supplementary Figure S1C) and subsequently generate the seed of the F₂ population in 2014. During 2015, the F₁ population, F₂ population, *Xinong 1B* (as wild-type) and the parent plants were grown in Chongqing, China. Mutated plants in the F₂ population (Supplementary Figure S1D) were used to locate the *NSG2* gene.

Morphological and histological analysis of *nsg2*

Among the field grown plants, we investigated the multiple defects of *nsg2* used *Xinong 1B* as the wild type control during different developmental stage.

At the booting stage (ca. 75 day after germination), the development process of early spikelets in *nsg2* mutants and wild-type plants were examined using a scanning electron microscope (SU3500, Hitachi, Tokyo, Japan) with a -20°C cool stage under a low-vacuum environment. At the flowering stage (~ 90 day after germination), the phenotypic characteristics of the mutant and wild-type spikelets were investigated using a scanning electron microscope (SU3500, Hitachi, Tokyo, Japan) and a NIKON SMZ1500 stereoscope (Nikon, Tokyo, Japan).

For paraffin section, mutant and wild-type spikelets at the heading stage were fixed in FAA (50% ethanol, 0.9 M glacial acetic and 3.7% formaldehyde) at 4°C for at least 16 h. A grade ethanol series was used to dehydrate the spikelets before they were infiltrated with xylene and then embedded in paraffin. $8\ \mu\text{m}$ -thick slices were cut (RM2245; Leica, Hamburg, Germany) and dyed sequentially with 1% safranin (Amresco) and 1% Fast Green (Amresco). Finally, the sections were mounted beneath a neutral balsam cover slip. Histological analysis was performed using the Nikon E600 microscope (Nikon, Tokyo, Japan).

Gene mapping of *NSG2*

The target gene was located according to the reported BSA method (Michelmore et al. 1991). DNA of the parents, F₂ population, normal and mutant gene pools were extracted from equal quantities of fresh leaf following the previously reported CTAB method with appropriate modifications (Murray and Thompson 1980). The quality and quantity of DNA were estimated using a NanoDrop 2000 spectrophotometer (Thermo Fisher Scientific, USA) and 1% agarose gel electrophoresis. SSR markers (<http://www.gramene.org/microsat/>) and IN/DEL markers from previous studies that distributed on the average of 12 chromosomes were employed for gene mapping. The primers we used were synthesized by the Shanghai Invitrogen Company, China.

The polymerase chain reaction (PCR) amplifications were carried out in a total volume of $15\ \mu\text{l}$, which contained $1.5\ \mu\text{l}$

10×PCR buffer, 1 μ l 50 ng μ l⁻¹ DNA, 0.75 μ l of 2.5 mmol⁻¹ dNTPs, 9.5 μ l ddH₂O, 1 μ l 10 mmol⁻¹ forward and reverse primer, and 0.25 μ l 5 U μ l⁻¹ rTaq DNA polymerase (TOYOBO, Japan). Amplification was performed with a MyCycler Thermal Cycler (Bio-Rad, CA, USA) under the following conditions: 5 min at 94°C for DNA strand separation, followed by 35 cycles of denaturing at 94°C for 30 s, annealing at 55°C for 30 s, extension at 72°C for 30 s, and finally extension at 72°C for 7 min. Amplified products were separated by electrophoresis on 10.0% polyacrylamide gels, before silver staining was undertaken to observe the color of the band patterns (Luo et al. 2007).

Linkage map construction

To analyze the results, the F₂ progeny expressing the band patterns of 56S and *Xinong 1B* were labeled A and B, and the heterozygote, which contained two parent bands, was labeled H. The linkage relationship was analyzed by MAPMAKER3.0 (Lander et al. 1987), and the recombination rate was transformed into genetic distance(cM) using the Kosambi mapping function. Meanwhile, we constructed a physical map based on the rice genome sequence information obtained from

the Gramene website (<http://www.gramene.org/>).

qPCR analysis

RNA from the lemma, palea and sterile lemma was isolated from the *nsg2* and wild-type plants using the RNAPrep Pure Plant Kit (Tiangen, Beijing, China). The first-strand cDNA was synthesized from 1 μ g of total RNA with oligo(dT)₁₈ primers in a 20 μ l reaction volume using the PrimeScript[®] Reagent Kit With gDNA Eraser (Takara, Dalian, China). The expression levels of floral specific genes (*OsMADS1*, *OsMADS6*, *OsMADS34*, and *DL*) (Table 1) were detected by qPCR. The qPCR analysis was performed using a SYBR premix Ex Taq II Kit (Takara, Dalian, China) in an ABI 7500 Sequence Detection System (Applied Biosystems, Carlsbad, CA, USA). *ACTIN* (*OsRac1*, *LOC_Os01g12900*) (Table 1) was used as an endogenous control. Three replicates were taken, and mean values for the expression of each gene were used in analysis.

Table 1. Primers used for qPCR analysis.

Primers	Forward sequence (5'-3')	Reverse sequence (5'-3')	Reference
<i>ACTIN</i>	GACCCAGATCATGTTTGAGACCT	CAGTGTGGCTGACACCATCAC	Ren et al. 2013
<i>OsMADS1</i>	TCTTGGTGAGGATTTGGGC	CCTTGCTCTTCAGATCAAACAG	Ren et al. 2013
<i>OsMADS6</i>	AGAGAAAGACGCAACTGATGATGG	AGGCTTGCTGCATGGCTCTG	Ren et al. 2013
<i>OsMADS34</i>	GCTTCGCAAGATGCTGCC	GTAGCCAGTGGAGCTAAATCCTC	Ren et al. 2013
<i>DL</i>	CCCATCTGCTTACAACCGCTT	GTTGGAGGTGGAACCGTCG	Ren et al. 2013

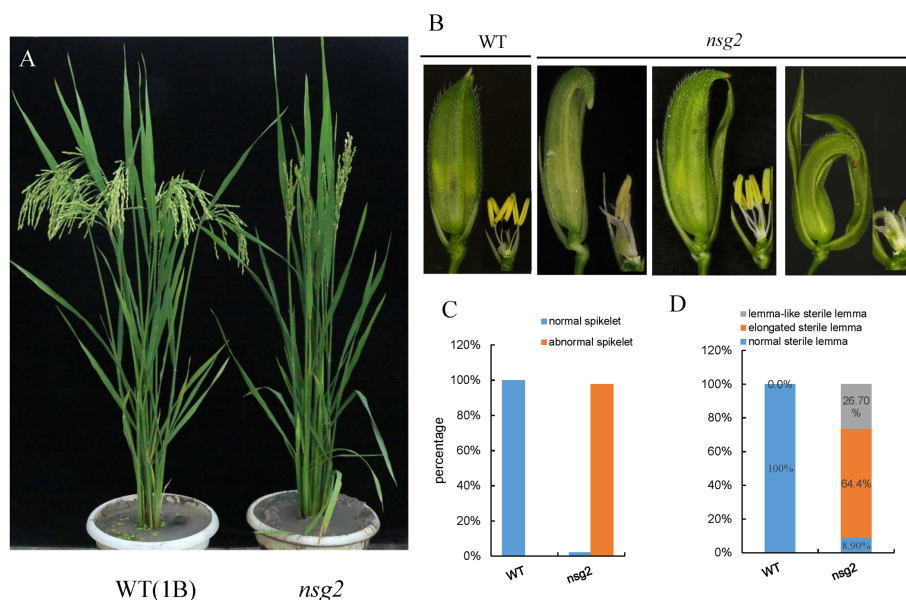


Figure 1. Phenotype and statistics of wild-type and *nsg2* plants. (A): The whole plant of wild-type and *nsg2*; (B): wild-type spikelets and *nsg2* spikelets with elongated/lemma-like sterile lemma; (C): phenotype statistics of normal spikelets (two rudimentary glumes are extremely degrade, two sterile lemmas are small and about 1/5 size of lemma, lemma is a little bigger than palea and hooked together with palea, enclosed the two lodicules, six stamens and a pistil) and abnormal spikelets (spikelets with one or more defects such as elongated rudimentary glume, elongated/lemma-like sterile lemma, degraded palea, decreased number of stamen) in wild-type and *nsg2*; (D): statistics of wild-type sterile lemma and sterile lemma of *nsg2* spikelet (normal, elongated and lemma-like sterile lemma).

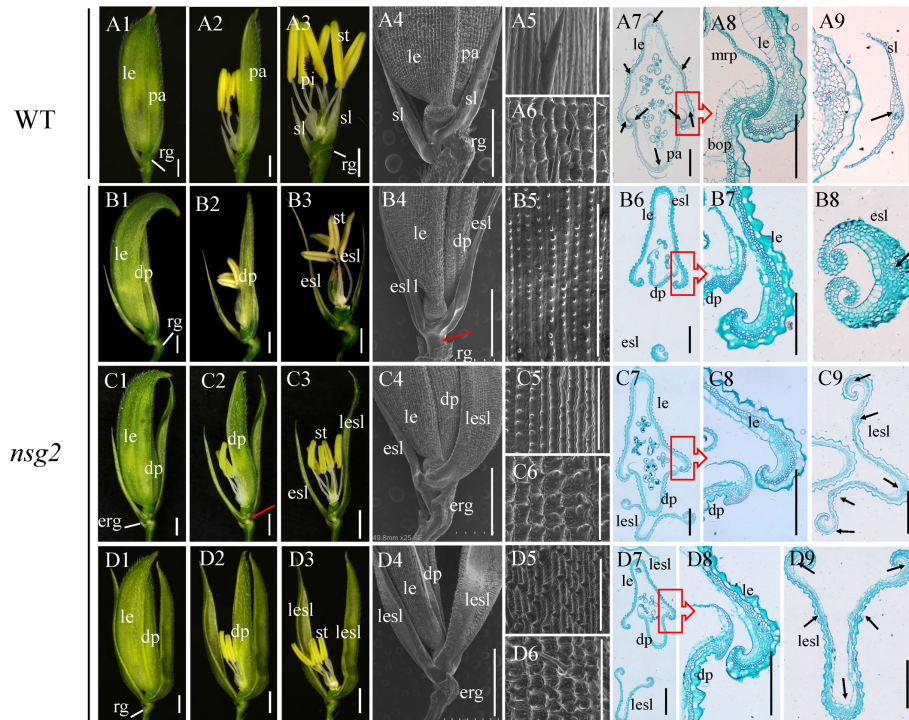


Figure 2. Phenotype of spikelets in the wild-type and *nsg2*. (A1–A3): Wild type spikelet; (A4): scanning electronic microscope analysis of spikelets in the wild type; (A5): epidermis of wild-type sterile lemma; (A6): epidermis of wild-type lemma; (A7–A9): histological analysis of spikelet in the wild type. A7: transverse section of wild spikelet; A8: magnified connection part of lemma and palea; A9: magnified wild-type sterile lemma; (B1–B3): *nsg2* spikelet with degraded palea; (B4): scanning electronic microscope analysis of *nsg2* spikelet with degraded palea; (B5): epidermis of elongated sterile lemma in *nsg2*; (B6–B8): histological analysis of *nsg2* spikelet with degraded palea. B6: Transverse section of *nsg2* spikelets with degraded palea and elongated sterile lemma; B7: magnified connection part of lemma and degraded palea; B8: magnified elongated sterile lemma; (C1–C3, D1–D3): *nsg2* spikelet with lemma-like sterile lemma; (C4, D4): scanning electronic microscope analysis of *nsg2* spikelet with lemma-like sterile lemma; (C5): epidermis of elongated sterile lemma in *nsg2* spikelet with one lemma-like sterile lemma and one elongated sterile lemma; (C6, D5–D6): epidermis of lemma-like sterile lemma in *nsg2*; (C7–C9, D7–D9): histological analysis of *nsg2* spikelet with lemma-like sterile lemma. C7, D7: transverse section of *nsg2* spikelet with lemma-like sterile lemma; C8, D8: magnified connection part of lemma and palea; C9, D9: magnified lemma-like sterile lemma. le: lemma; pa: palea; dp: degraded palea; st: stamen; pi: rudimentary glume; erg: elongated rudimentary glume; sl: sterile lemma; esl: elongated sterile lemma; lesl: lemma-like sterile lemma; black arrows represent the vascular bundles; red arrow represents elongated rachilla axis; red box with arrow in A7, B6, C7, D7 represents the unmagnified part of A8, B7, C8, D8. Bars=1,000 μm in A1–A6, B1–B5, C1–C6, D1–D6 and 250 μm in A7–A9, B7–B9, C7–C9, D7–D9.

Results

Morphological and histological analysis of *nsg2* mutants

During the vegetative stage, no significant difference was observed between the *nsg2* mutant and the wild-type plants, however, the *nsg2* mutant exhibited remarkable abnormalities in spikelet development (Figure 1A, B). In *nsg2* panicle, there were about 97.8% spikelets displaying defective features (including elongated/lemma-like sterile lemma, elongated rudimentary glume, degraded palea and decreased stamen) (Figure 1C).

Generally, a wild-type rice spikelet is composed of a top fertile floret and a pair of sterile lemmas and a pair of rudimentary glumes (Figure 2A1–A3). The sterile lemmas are two lamella-like organs and is only about 1/5 the size of the lemma. And the sterile lemma had a smooth adaxial surface with a few trichomes (Figure 2A4–A5). The rudimentary glume is extremely degenerated (Figure 2A1, A4). The floret includes four

whorls of floral organs: one lemma and one palea in whorl 1, two lodicules in whorl 2, six stamens in whorl 3, and one pistil that forms the fourth whorl. The stamen is composed of a filament and an anther, and the pistil is composed of one ovary and two stigmas (Figure 2A1–A3). Lemma and palea enclose the internal three whorls of floral organs, and develop a silicified adaxial epidermis bearing trichomes and protrusions (Figure 2A4, A6, A8).

In 26.7% spikelets of *nsg2*, elongation of the sterile lemma was observed (Figures 1D, 2B1–B3). The elongated sterile lemma was longer than the wild-type sterile lemma, and developed some silicified cells on the adaxial epidermis (Figure 2B4, B5). In 64.4% spikelets of *nsg2*, the sterile lemmas were larger than that in the wild-type spikelets and resembling the lemma. The palea also displayed degeneration to different degrees (Figures 1D, 2C1, D1). Epidermis of the lemma-like sterile lemma was covered with silicified cells, which wasn't produced on the sterile lemma of wild-type (Figure 2C4, C6, D4–D6). In a small part of the spikelets, the rudimentary glumes

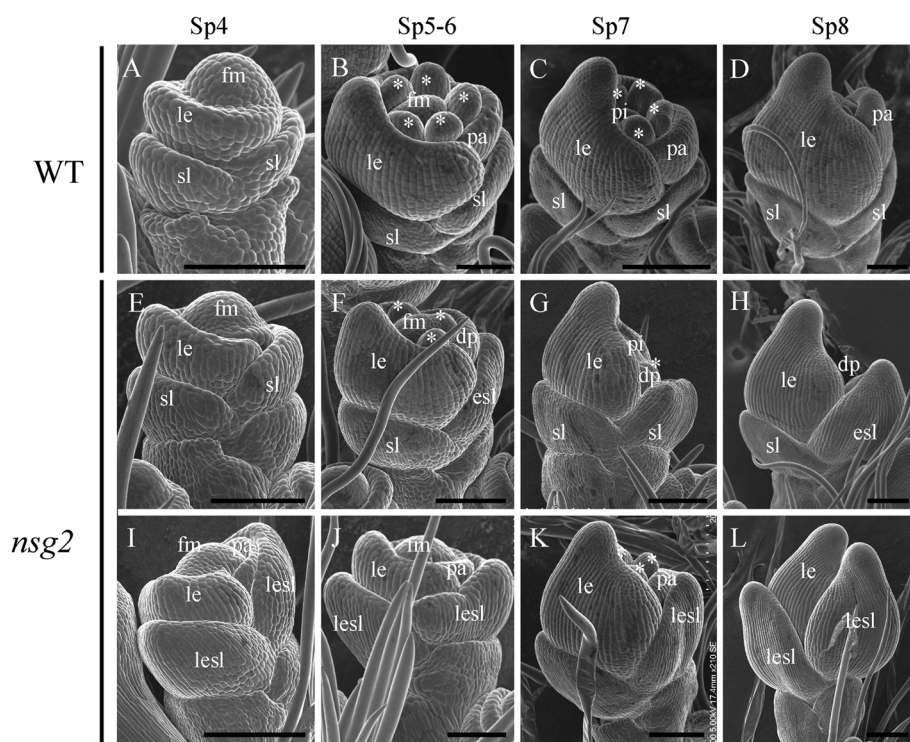


Figure 3. Scanning electron micrographs of florets at early developmental stages in the wild type and *nsg2*. (A–D): Wild type spikelets; (E–H): *nsg2* spikelets with degraded palea; (I–L): *nsg2* spikelets with elongated lemma-like sterile lemma; fm: floral meristem; sl: sterile lemma; esl: elongated sterile lemma; lesl: lemma-like sterile lemma; le: lemma; pa: palea; dp: degraded palea; pi: pistil; *: stamens. Bars=100 μ m.

were elongated (Figure 2B4, C1–C3), and the rachilla also showed elongation to some extent (Figure 2C1–C4). In addition, the number of stamens in some florets was reduced to between two and five (Figure 2B6, C7, D7).

Micromorphological and histological analysis was also performed. In the wild-type, the lemma was hooked with palea (Figure 2A7) and developed five vascular bundles, which marked by black arrows in the transverse section of spikelet (Figure 2A7). In contrast to the lemma, the palea consisted of two parts: the body of palea (bop) and the marginal region of palea (mrp) and developed three vascular bundles (Figure 2A7–A8). Both the bop and the lemma had four cell layers: a silicified outer epidermal cell layer, a fibrous sclerenchyma cell layer, a spongy parenchymatous cell layer, and an inner epidermal cell layer. There was an abundance of spongy tissue but few sclerenchyma cells in the mrp between the two smooth epidermal cell layers (Figure 2A8). The sterile lemma had smooth epidermal cells with parenchyma cells, and one vascular bundle in the middle (Figure 2A9). In the *nsg2* mutant, the cell structure of these elongated sterile lemmas was similar to that in the lemma and bop to differing degrees (Figure 2B8, C7, C9, D7, D9). In some sterile lemma, the degree of silicification in the outer epidermal cell layer was lower, and the number of vascular bundles was not increased, although an obvious fibrous cell layer was found (Figure 2B8). In other sterile lemmas, the cell structure was completely

consistent with the lemma: it contained the outer epidermal cell layer with a high degree of silicification, five vascular bundles, obvious fibrous sclerenchyma, and a spongy parenchymatous cell layer (Figure 2C9, D9). These results indicate that the elongated sterile lemma had transformed into a lemma-like organ. In addition, the cell structure in the *nsg2* palea showed no obvious difference from that in the wild-type, but it did become smaller on the whole. This led to the non-closure of the lemma and the palea (Figure 2B6, B7, C7, C8, D7, D8).

Micromorphological analysis of nsg2 at early stage of flower development

We examined young spikelets of the wild-type and mutant plants at early developmental stages using scanning electron microscopy (SEM). The development progress of the sterile lemma in the *nsg2* mutant was significantly different from that in the wild-type. In the wild-type, the spikelet development is categorized into eight stages (Sp1–Sp8) based on the identity of lateral organs (Ikeda et al. 2004). At Sp2 stage, a pair of sterile lemmas is formed in 1/2 alternate arrangement, and during Sp3–Sp5 stage, the sterile lemmas continue growing and elongated. (Figure 3A, B). In the *nsg2* mutant, the growth rate of the sterile lemma was significantly faster than that in the wild-type, and the sterile lemma continued to elongate during Sp6–Sp8. Some *nsg2* sterile lemmas were very similar to the

lemma in size, shape, and development progress during these stages (Figure 3E–L). The results showed that the development of the sterile lemma in the *nsg2* mutant displayed a development process similar to that of the lemma; in other words, the mutation of the *NSG2* gene resulted in the homeoetic transformation of the sterile lemma primordia into the lemma primordia at the early stage of flower development.

Some defects in the floral organ primordia were also observed in the *nsg2* mutant. In the wild-type spikelets, the palea primordia is formed at a 180° position apart from the lemma during the Sp4 stage (Figure 3A). During Sp5–6 stage, the lodicule and stamen primordias are formed, but only stamen primordias could be observed (Figure 3B). During Sp7 stage, the carpel primordia and the palea continued to differentiate, the marginal region of the palea began to hook with the lemma (Figure 3C). During Sp8 stage, the ovule and pollens developed, palea and lemma close together (Figure 3D). However, during the same stage in the *nsg2* mutant, the palea generally developed slower than in the wild-type, and the palea primordia was significantly smaller than the normal palea primordia in Sp7 and Sp8 (Figure 3G, H). Moreover, the initiation of stamens was not synchronized and was later than in the wild-type, and the number of stamens was significantly reduced (Figure 3F, G, J, K). Entering the Sp8 stage, the lemma and palea of the wild-type were closed and wrapped the inner organs. However, in the *nsg2* mutant, as a result of the delayed development of the palea, the lemma and palea could not be closed (Figure 3H, L).

Expression analysis of floral organ identity genes in the sterile lemma of *nsg2* and wild-type spikelets

To clarify the identity of this elongated sterile lemma precisely, we examined the expression levels of *OsMADS1*, *OsMADS6*, *OsMADS34*, and *DL* in the lemma, palea normal sterile lemma (not elongated sterile lemma), elongated sterile lemma and lemma-like sterile lemma of *nsg2* spikelets and lemma, palea, sterile lemma of wild-type spikelets (Figure 4A–D). In the wild-type spikelets, *OsMADS1* gene had a high level of expression in the lemma and the palea, and a very low expression in the sterile lemma (Figure 4B). *OsMADS6* strongly expressed in the palea, but nearly not expressed in the sterile lemma or lemma (Figure 4C). And *DL* gene strongly expressed in the lemma, but not in the palea or sterile lemma (Figure 4D). In the *nsg2* mutant, high levels of expression of *OsMADS1* and *DL* were detected in the lemma-like sterile lemma, while only a low level of expression was detected in the elongated sterile lemma and normal sterile lemma (Figure 4B, D). Moreover, only extremely low or nearly no expression of *OsMADS6* was detected in the normal/elongated/lemma-like sterile

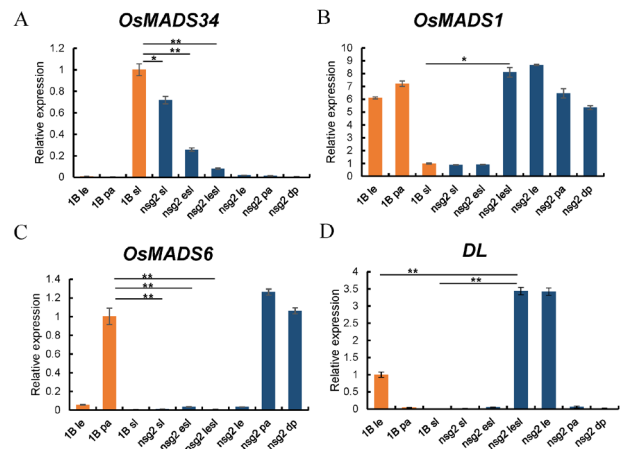


Figure 4. qPCR analysis of *OsMADS1*, *OsMADS6*, *OsMADS34* and *DL* in *nsg2* and wild-type. sl: Sterile lemma; le: lemma; pa: palea; esi: elongated sterile lemma; lesl: lemma-like sterile lemma; dp: degraded palea. Error bars represent the standard deviation between three replicates in the qPCR data; * indicates a statistically significant difference ($p < 0.05$); ** indicates a statistically significant difference ($p < 0.01$).

lemma (Figure 4C). In the wild-type, *OsMADS34* was highly expressed in the sterile lemma, but not in the lemma or palea (Figure 4A). In the *nsg2* spikelets, the expression of *OsMADS34* in the lemma and palea was similar to that of wild-type spikelets. However, there was a decreased expression of *OsMADS34* in three types of sterile lemma: normal sterile lemma, elongated sterile lemma and lemma-like sterile lemma. And expression of *OsMADS34* in the lemma-like sterile lemma was obviously lower than the normal and elongated sterile lemma (Figure 4A). These results indicate that the lemma-like sterile lemma had gained the identity of the lemma, and further suggest that the *NSG2* gene plays a key role in the regulation of the identity genes of these floral organs.

Genetic analysis of *nsg2*

The *nsg2* mutant was crossed with the sterile line 56S to yield the F_1 population. All F_1 plants exhibited a normal phenotype. In the F_2 population, the segregation ratio of normal to mutant phenotypes was 3:1 ($\chi^2 = 2.57 < \chi_{0.05}^2 = 3.84$). This result indicates that the *nsg2* trait was controlled by a single recessive gene.

Gene mapping of *NSG2*

To map the *NSG* gene, the 676 mutant plants in the F_2 population were used as a mapping population. 10 normal plants and 10 mutant plants, randomly selected from the F_2 segregating population were used to construct the normal and the mutant gene pool. Then the 102 pairs of markers that showed polymorphism between two parents were employed to screen the normal and mutant gene pool. Four markers, ZTQ65, ZTQ66, CY7-6, and CY7-15 on chromosome 7, showed polymorphism

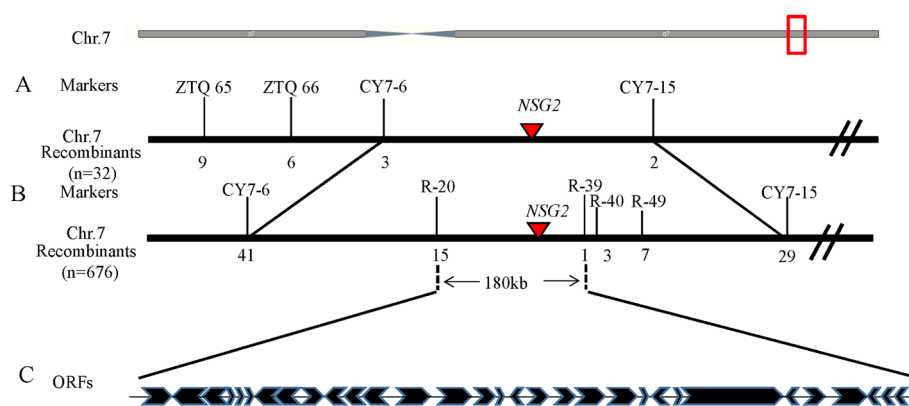


Figure 5. Linkage map among *NSG2* and markers on chromosome 7 in rice. (A): Preliminary mapping of *NSG2*; (B): fine mapping of *NSG2*; (C): annotated genes in the mapping region.

Table 2. Polymorphic markers used for gene mapping.

Primers	Forward sequence (5'-3')	Reverse sequence (5'-3')	Physical location
CY7-6	ACTGCCAAAGATGTGAAGCTAA	AATTCACCTTTGGAAACAATGGA	7.25691751
CY7-15	TCGCTCGTCAATTCTCTCCAC	ATGCATAATACGGAGTAGTGAAC	7.27399714
R20	CGTTGAGACGGTCACCTAATGC	GCTCAAATGTTTGACACGAAGC	7.26286113
R34	CCAGTTTATCTTCTGCACCTTCTCG	TCTTTGAGCAGATGGCTAACCAAGG	7.26351074
R37	AATGGAGGTGCGATACATTCTGC	GATATATGCATAAGCGGTGTGTGG	7.26404613
R39	GATCAACGAACCCACCACACC	CGCGTCTTGTATATGCACTTGATCC	7.26461929
R40	AATGGAGCTCCTGACTCTAAAGC	TGCATCTCCTACAGAAACAAGG	7.26465820
R49	GGTCACTAAATACCATGAGGATACCG	AGATCGAGGCCTATCCGATCC	7.26670489
ZTQ65	CCATCGTGCTGATGCTCC	TCGAGTGGCGTAGTCTAGTCG	7.21146340
ZTQ66	ACACCAGCCATCACCTGTTAC	GAGTAAGAGCGGGCTGGC	7.23628080

Table 3. Annotated genes in the mapping region.

Gene ID	Describes	Gene ID	Describes
<i>LOC_Os07g43970</i>	calmodulin-binding protein, putative, expressed	<i>LOC_Os07g44120</i>	hypothetical protein
<i>LOC_Os07g43980</i>	DEAD-box ATP-dependent RNA helicase, putative, expressed	<i>LOC_Os07g44130</i>	cytochrome P450 72A1, putative, expressed
<i>LOC_Os07g43990</i>	expressed protein	<i>LOC_Os07g44140</i>	cytochrome P450 72A1, putative, expressed
<i>LOC_Os07g44000</i>	expressed protein	<i>LOC_Os07g44160</i>	retrotransposon protein, putative, unclassified, expressed
<i>LOC_Os07g44004</i>	expressed protein	<i>LOC_Os07g44170</i>	pentatricopeptide repeat domain containing protein, putative, expressed
<i>LOC_Os07g44010</i>	expressed protein	<i>LOC_Os07g44180</i>	OsRCI2-10-Hydrophobic protein LTI6A, expressed
<i>LOC_Os07g44020</i>	SNARE associated Golgi protein, putative, expressed	<i>LOC_Os07g44190</i>	h/ACA ribonucleoprotein complex subunit 4, putative, expressed
<i>LOC_Os07g44030</i>	myb/SANT domain protein, putative, expressed	<i>LOC_Os07g44200</i>	transcription regulator, putative, expressed
<i>LOC_Os07g44040</i>	ras-related protein, putative, expressed	<i>LOC_Os07g44210</i>	SNF2 family N-terminal domain containing protein, expressed
<i>LOC_Os07g44050</i>	expressed protein	<i>LOC_Os07g44220</i>	expressed protein
<i>LOC_Os07g44060</i>	haloacid dehalogenase-like hydrolase family protein, putative, expressed	<i>LOC_Os07g44230</i>	ribosomal protein L7Ae/L30e/S12e/Gadd45 family protein, putative, expressed
<i>LOC_Os07g44070</i>	pectinacetyltransferase domain containing protein, expressed	<i>LOC_Os07g44240</i>	transposon protein, putative, unclassified, expressed
<i>LOC_Os07g44080</i>	expressed protein	<i>LOC_Os07g44250</i>	dirigent, putative, expressed
<i>LOC_Os07g44090</i>	myb-related protein Hv33, putative, expressed	<i>LOC_Os07g44260</i>	dirigent, putative, expressed
<i>LOC_Os07g44100</i>	expressed protein	<i>LOC_Os07g44280</i>	dirigent, putative, expressed
<i>LOC_Os07g44110</i>	cytochrome P450 72A1, putative, expressed		

between the two DNA pools. Then we use 32 mutant individuals to verify the linkage of the four markers, the number of recombinants of ZTQ65, ZTQ66, CY7-6 decreased gradually (9, 6, 3) and did not overlap with the 2 recombinants of CY7-15. The results revealed that *NSG2* was located between IN/DEL markers CY7-6 and CY7-15 on the long arm of chromosome 7, with 3 and 2

recombinants (Figure 5A; Supplementary Figure S2).

Next, the two IN/DEL markers CY7-6 and CY7-15 were used to survey the whole 676 mutant individuals and found 41 and 29 recombinants, respectively. In order to further locate *NSG2*, 21 pairs of SSR primers between CY7-6 and CY7-15 were synthesized. Of these primers, R-20, R-34, R-37, R-39, R-40, and R-49 exhibited

polymorphism (Table 2). These six pairs of primers were used to further analyze all the 70 recombinants. The results showed that each marker had 15, 0, 0, 1, 3, 7 recombinants (Supplementary Figure S3). Finally, the *NSG2* gene was located between the SSR markers R-20 and R-39, with an approximate 180 kb physical distance in the genome sequencing variety *Nipponbare* (Figure 5B). According to the gene annotation information provided by the Gramene website (http://www.gramene.org/Oryza_sativa/Location/), we found that there were 31 annotated genes in the mapping region (Figure 5C), including eight expressed proteins, four putative proteins, three cytochrome proteins, two MYB proteins, two transposon proteins, one transcription regulator, and several functional proteins (Table 3).

Discussion

In rice, more and more studies provide direct or indirect evidence for the hypothesis which states that a spikelet of *Oryza* originally contained a terminal floret and two lateral florets, and that the two lateral florets subsequently degenerated during evolution, leaving only the lemma (Kellogg 2009). The sterile lemma seems to be derived from the degeneration of this lemma (Kobayashi et al. 2010; Yoshida et al. 2009). In *g1*, *eg1*, *osmads34*, *asp1*, *nsg*, *dg1* mutants and *OsMADS1* ectopic expression plants, the sterile lemma homeotic transformed into lemma-like organ suggest that the sterile lemma and lemma were homologous organs, thus partly support the above hypothesis (Gao et al. 2010; Kobayashi et al. 2010, 2012; Li et al. 2009; Liu et al. 2016; Wang et al. 2013; Yoshida et al. 2009, 2012). In *lateral floret 1* (*lf1*) mutant, the spikelet of *lf1* developed lateral florets with proper floral organ identities in the axil of the sterile lemma (Zhang et al. 2017). Furthermore, two florets within a single spikelet were observed in the two allelic mutants *double floret1-1* (*df1-1*) and *df1-2*, and each single floret developed four whorls of floral organs. Three florets were also observed, though this was much less common (Ren et al. 2018). These studies constitute much stronger evidence in support of the three-florets spikelet hypothesis. In our research, the *nsg2* mutant developed a lemma-like sterile lemma in a similar way to *g1*, *eg1*, *osmads34*, *asp1*, *nsg*, *dg1* mutants, and *OsMADS1* ectopic expression plants. However, the difference was that the elongated sterile lemmas in *g1*, *eg1*, *osmads34*, *asp1*, *nsg* mutants, and *OsMADS1* ectopic expression plants all developed similarly to lemma in shape and identity, while no identity of palea was observed. In the sterile lemma of *nsg2*, the expression signals of both lemma identity genes were detected, indicating that the elongated sterile lemma may obtain the identities of lemma. This result provides partial evidence for the hypothesis of the evolution of the sterile lemma. The *NSG2* gene plays a key role in

maintaining sterile lemma identity by repressing the identity of the lateral floret and lateral remaining lemma during the evolution of rice. Moreover, increasing rice yield has always been the main goal of rice breeding. In addition to increasing the number of primary and secondary branches, increasing the number of florets in spikelet is also an important way to increase rice yield. Together with the previous researches, the sterile lemma of *nsg2* transformed into lemma-like organ provides evidence to support “three-florets spikelet” hypothesis, which indicate that it is possible to cultivated a “three-florets spikelet” rice. If succeed, the number of grains per panicle would be dramatically increased and affect rice yield.

The lemma and palea are unique floral organs in grass plants, with different origins and characteristics. The palea is generally considered to be the first leaf on the flower axis and the lemma is the bract (Kellogg 2009; Ohmori et al. 2009). In rice, the palea is an organ produced by the congenital fusion of the bop (the body of palea) and the mrp (the marginal region of palea), which potentially have distinct origins (Lombardo and Yoshida 2015; Yoshida and Nagato 2011). The cellular structure of the bop has been shown to be highly similar to that of the lemma but distinct from that of the mrp (Cusick 1966; Verbeke 1992; Zanis 2007). In previous studies, several mutants have also exhibited a degraded palea: genes *DP1*, *REP1*, *PD1* and *DEP/OsMADS15* greatly affect the structure of the palea. In the *depressed palea 1* (*dp1*) mutant, the body of the palea is destroyed and finally turned into a leaf-like organ comprising just the margin of the palea (Jin et al. 2011; Luo et al. 2005). In the *dense and erect panicle1* (*dep1*) and the *retarded palea* (*rep*) mutants, the body of the palea is severely degraded, but the margin structure is widened (Wang et al. 2010; Yuan et al. 2009; Zeng et al. 2016). The *palea defective 1* (*pd1*) mutant shows a smaller and flatter leaf-like palea, which causes the lemma to bend excessively inwards (Xiang et al. 2015). *cy15* is a novel mutation in the C terminus of *OsMADS1* and the development of the palea in severe *cy15* spikelets is greatly affected: the size of bop is reduced, whereas the mrps are normal (Zhang et al. 2018). The results are in accordance with the view that the palea is a chimeric organ, and that the identities of bop and mrp are controlled by different regulatory pathways. In the *nsg2* mutant, the palea degenerated to varying degrees and led to the non-closure of the lemma and palea, while the identity of the lemma remained normal. In addition, the palea of *nsg2* was reduced with a smaller bop, while the identities of bop and mrp were unchanged. In other words, *NSG2* may regulate cell proliferation and expansion to maintain the size of the palea, but it does not affect its identity.

In this study, *NSG2* gene was mapped on chromosome 7, with a 180-kb region in *Nipponbare*. In the region,

we didn't find known genes involved in spikelet development. Therefore, *NSG2* was a new gene involving the sterile lemma development.

Among those 31 annotated genes in the mapping region, there are two MYB family transcription factors: *LOC_Os07g44030* and *LOC_Os07g44090*. Previous studies have shown that MYB transcription factors exist in almost all plants and are involved in the development of the floral organs. In *Arabidopsis*, *AtMYB21* and *AtMYB24* influence JA metabolism through interactions with JAZ, thus regulating stamen development. *myb21* and *myb24* mutants showed defects in pollen maturation, anther cracking and fiber elongation, which eventually led to male sterility (Cheng et al. 2009; Song et al. 2011). In *atmyb26* mutant, the anther could not crack and disperse pollen because there was no secondary thickening of the cells in the wall of the drug chamber (Dawson et al. 1999). In rice, *ANTHER INDEHISCENCE1 (AID1)*, encodes a 1R-MYB protein. Loss of function of *AID1* leads to pollen abortion and delayed anthesis (Zhu et al. 2004). *OsGAMYB* and *CARBON STARVED ANTHEP (CSA)* are both R2R3 MYB transcription factor, and regulate the development of pollen (Aya et al. 2009; Kaneko et al. 2004; Zhu et al. 2015). Interestingly, *COP1* is a negative regulator of light morphogenesis, ectopically expressed *AtMYB24* in *cop1* leads to narrowed petals and deformed carpels (Shin et al. 2002). Those researches showed that MYB factors played an important role in flower development. Therefore, the two MYB family factors *LOC_Os07g44030* and *LOC_Os07g44090* in the mapping region might be involved in the development of the spikelet and floral organ. And they were considered as the candidate genes of *NSG2*. Our next step will be to carry out further identification and cloning of these two genes to confirm the identity of *NSG2*.

Acknowledgements

This work was supported by the National Natural Science Foundation of China (31730063, 31271304), National Key Program for Research and Development (2017YFD0100202), Project of CQ CSTC (CSTC2017jcyjBX0062), Graduate student scientific research innovation projects in Chongqing (CYS2015066), and the Fundamental Research Funds for the Central Universities (XDJK2016A013).

References

- Agrawal GK, Abe K, Yamazaki M, Miyao A, Hirochika H (2005) Conservation of the E-function for floral organ identity in rice revealed by the analysis of tissue culture-induced loss-of-function mutants of the *OsMADS1* gene. *Plant Mol Biol* 59: 125–135
- Ashikari M, Sakakibara H, Lin SY, Yamamoto T, Takashi T, Nishimura A, Angeles ER, Qian Q, Kitano H, Matsuoka M (2005) Cytokinin oxidase regulates rice grain production. *Science* 309: 741–745
- Aya K, Ueguchi-Tanaka M, Kondo M, Hamada K, Yano K, Nishimura M, Matsuoka M (2009) Gibberellin modulates anther development in rice via the transcriptional regulation of *GAMYB*. *Plant Cell* 21: 1453–1472
- Cheng H, Song S, Xiao L, Soo HM, Cheng Z, Xie D, Peng J (2009) Gibberellin acts through jasmonate to control the expression of *MYB21*, *MYB24*, and *MYB57* to promote stamen filament growth in *Arabidopsis*. *PLoS Genet* 5: e1000440
- Cusick F (1966) On phylogenetic and ontogenetic fusions. In: Gutter EG (ed) *Trends in Plant Morphogenesis*. Longmans, London, pp 170–183
- Dawson J, Sözen E, Vizir I, Van Waeyenberge S, Wilson ZA, Mulligan BJ (1999) Characterization and genetic mapping of a mutation (*ms35*) which prevents anther dehiscence in *Arabidopsis thaliana* by affecting secondary wall thickening in the endothecium. *New Phytol* 144: 213–222
- Gao X, Liang W, Yin C, Ji S, Wang H, Su X, Guo C, Kong H, Xue H, Zhang D (2010) The SEPALLATA-Like gene *OsMADS34* is required for rice inflorescence and spikelet development. *Plant Physiol* 153: 728–740
- Hong L, Qian Q, Zhu K, Tang D, Huang Z, Gao L, Li M, Gu M, Cheng Z (2010) ELE restrains empty glumes from developing into lemmas. *J Genet Genomics* 37: 101–115
- Ikeda K, Sunohara H, Nagato Y (2004) Developmental course of inflorescence and spikelet in rice. *Breed Sci* 54: 147–156
- Jin Y, Luo Q, Tong H, Wang A, Cheng Z, Tang J, Li D, Zhao X, Li X, Wan J, et al. (2011) An AT-hook gene is required for palea formation and floral organ number control in rice. *Dev Biol* 359: 277–288
- Kaneko M, Inukai Y, Ueguchi-Tanaka M, Itoh H, Izawa T, Kobayashi Y, Hattori T, Miyao A, Hirochika H, Ashikari M, et al. (2004) Loss-of-function mutations of the rice *GAMYB* gene impair α -amylase expression in aleurone and flower development. *Plant Cell* 16: 33–44
- Kellogg EA (2009) The evolutionary history of Ehrhartoideae, Oryzaceae, and *Oryza*. *Rice (NY)* 2: 1–14
- Kobayashi K, Maekawa M, Miyao A, Hirochika H, Kyojuka J (2010) *PANICLE PHYTOMER2 (PAP2)*, encoding a SEPALLATA subfamily MADS-box protein, positively controls spikelet meristem identity in rice. *Plant Cell Physiol* 51: 47–57
- Kobayashi K, Yasuno N, Sato Y, Yoda M, Yamazaki R, Kimizu M, Yoshida H, Nagamura Y, Kyojuka J (2012) Inflorescence meristem identity in rice is specified by overlapping functions of three AP1/FUL-Like MADS box genes and *PAP2*, a SEPALLATA MADS box gene. *Plant Cell* 24: 1848–1859
- Kwon Y, Yu SI, Park JH, Li Y, Han JH, Alavilli H, Cho JJ, Kim TH, Jeon JS, Lee BH (2012) *OsREL2*, a rice TOPLESS homolog functions in axillary meristem development in rice inflorescence. *Plant Biotechnol Rep* 6: 213–224
- Lander ES, Green P, Abrahamson J, Barlow A, Daly MJ, Lincoln SE, Newberg LA (1987) MAPMAKER: An interactive computer package for constructing primary genetic linkage maps of experimental and natural populations. *Genomics* 1: 174–181
- Li F, Liu W, Tang JY, Chen JF, Tong HN, Hu B, Li CL, Fang J, Chen MS, Chu CC (2010) Rice *DENSE AND ERECT PANICLE 2* is essential for determining panicle outgrowth and elongation. *Cell Res* 20: 838–849
- Li H, Xue D, Gao Z, Yan M, Xu W, Xing Z, Huang D, Qian Q, Xue Y (2009) A putative lipase gene *EXTRA GLUME1* regulates both empty-glume fate and spikelet development in rice. *Plant J* 57: 593–605

- Liu M, Li H, Su Y, Li W, Shi C (2016) *G1/ELE* functions in the development of rice lemmas in addition to determining identities of empty glumes. *Front Plant Sci* 7: 1006
- Lombardo F, Yoshida H (2015) Interpreting lemma and palea homologies: A point of view from rice floral mutants. *Front Plant Sci* 6: 61
- Luo Q, Zhou K, Zhao X, Zeng Q, Xia H, Zhai W, Xu J, Wu X, Yang H, Zhu L (2005) Identification and fine mapping of a mutant gene for paleales spikelet in rice. *Planta* 221: 222–230
- Luo Z, Yang Z, Zhong B, Li Y, Xie R, Zhao F, Ling Y, He G (2007) Genetic analysis and fine mapping of a dynamic rolled leaf gene, *RL10(t)*, in rice (*Oryza sativa* L.). *Genome* 50: 811–817
- McSteen P, Laudencia-Chingcuanco D, Colasanti J (2000) A floret by any other name: Control of meristem identity in maize. *Trends Plant Sci* 5: 61–66
- Michelmore RW, Paran I, Kesseli RV (1991) Identification of markers linked to disease-resistance genes by bulked segregant analysis: A rapid method to detect markers in specific genomic regions by using segregating populations. *Proc Natl Acad Sci USA* 88: 9828–9832
- Miura K, Ikeda M, Matsubara A, Song XJ, Ito M, Asano K, Matsuoka M, Kitano H, Ashikari M (2010) *OsSPL14* promotes panicle branching and higher grain productivity in rice. *Nat Genet* 42: 545–549
- Murray MG, Thompson WF (1980) Rapid isolation of high molecular weight plant DNA. *Nucleic Acids Res* 8: 4321–4326
- Ohmori S, Kimizu M, Sugita M, Miyao A, Hirochika H, Uchida E, Nagato Y, Yoshida H (2009) *MOSAIC FLORAL ORGANS1*, an AGL6-Like MADS box gene, regulates floral organ identity and meristem fate in rice. *Plant Cell* 21: 3008–3025
- Prasad K, Parameswaran S, Vijayraghavan U (2005) *OsMADS1*, a rice MADS-box factor, controls differentiation of specific cell types in the lemma and palea and is an early-acting regulator of inner floral organs. *Plant J* 43: 915–928
- Prasad K, Sriram P, Kumar SC, Kushalappa K, Vijayraghavan U (2001) Ectopic expression of rice *OsMADS1* reveals a role in specifying the lemma and palea, grass floral organs analogous to sepals. *Dev Genes Evol* 211: 281–290
- Ren D., Li Y, Zhao F, Sang X, Shi J, Wang N, Guo S, Ling Y, Zhang C, Yang Z, et al. (2013) MULTI-FLORET SPIKELET1, which encodes an AP2/ERF protein, determines spikelet meristem fate and sterile lemma identity in rice. *Plant Physiol* 162: 872–884
- Ren D, Yu H, Rao Y, Xu Q, Zhou T, Hu J, Zhang Y, Zhang G, Zhu L, Gao Z, et al. (2018) ‘Two-floret spikelet’ as a novel resource has the potential to increase rice yield. *Plant Biotechnol J* 16: 351–353
- Schmidt RJ, Ambrose BA (1998) The blooming of grass flower development. *Curr Opin Plant Biol* 1: 60–67
- Shin B, Choi G, Yi H, Yang S, Cho I, Kim J, Lee S, Paek NC, Kim JH, Song PS, et al. (2002) *AtMYB21*, a gene encoding a flower-specific transcription factor, is regulated by *COPI*. *Plant J* 30: 23–32
- Song S, Qi T, Huang H, Ren Q, Wu D, Chang C, Peng W, Liu Y, Peng J, Xie D (2011) The jasmonate-ZIM domain proteins interact with the R2R3-MYB transcription factors *MYB21* and *MYB24* to affect jasmonate-regulated stamen development in Arabidopsis. *Plant Cell* 23: 1000–1013
- Terrell EE, Peterson PM, Wergin WP (2001) *Epidermal Features and Spikelet Micromorphology in Oryza and Related Genera (Poaceae: Oryzaceae)*. Smithsonian Institution Press, Washington, D.C.
- Verbeke JA (1992) Fusion events during floral morphogenesis. *Annu Rev Plant Physiol Plant Mol Biol* 43: 583–598
- Wang K, Tang D, Hong L, Xu W, Huang J, Li M, Gu M, Xue Y, Cheng Z (2010) *DEP* and *AFO* regulate reproductive habit in rice. *PLoS Genet* 6: e1000818
- Wang L, Zeng XQ, Zhuang H, Shen YL, Chen H, Wang ZW, Long JC, Ling YH, He GH, Li YF (2017) Ectopic expression of *OsMADS1* caused dwarfism and spikelet alteration in rice. *Plant Growth Regul* 81: 433–442
- Wang N, Li Y, Sang X, Ling Y, Zhao F, Yang Z, He G (2013) *Nonstop glumes (nsg)*, a novel mutant affects spikelet development in rice. *Genes Genomics* 35: 149–157
- Xiang C, Liang X, Chu R, Duan M, Cheng J, Ding Z, Wang J (2015) Fine mapping of a *palea defective 1 (pd1)*, a locus associated with palea and stamen development in rice. *Plant Cell Rep* 34: 2151–2159
- Xue W, Xing YZ, Weng XY, Zhao Y, Tang WJ, Wang L, Zhou HJ, Yu SB, Xu CG, Li XH, et al. (2008) Natural variation in *Ghd7* is an important regulator of heading date and yield potential in rice. *Nat Genet* 40: 761–767
- Yan CJ, Zhou XH, Yan S, Chen F, Yeboah M, Tang SZ, Liang GH, Gu MH (2007) Identification and characterization of a major QTL responsible for erect panicle trait in japonica rice (*Oryza sativa* L.). *Theor Appl Genet* 115: 1093–1100
- Yoshida A, Ohmori Y, Kitano H, Taguchi-Shiobara F, Hirano HY (2012) *ABERRANT SPIKELET AND PANICLE1*, encoding a TOPLESS-related transcriptional co-repressor, is involved in the regulation of meristem fate in rice. *Plant J* 70: 327–339
- Yoshida A, Suzaki T, Tanaka W, Hirano HY (2009) The homeotic gene *long sterile lemma (G1)* specifies sterile lemma identity in the rice spikelet. *Proc Natl Acad Sci USA* 106: 20103–20108
- Yoshida H, Nagato Y (2011) Flower development in rice. *J Exp Bot* 62: 4719–4730
- Yuan Z, Gao S, Xue DW, Luo D, Li LT, Ding SY, Yao X, Wilson ZA, Qian Q, Zhang DB (2009) *RETARDED PALEA1* controls palea development and floral zygomorphy in rice. *Plant Physiol* 149: 235–244
- Zanis MJ (2007) Grass spikelet genetics and duplicate gene comparisons. *Int J Plant Sci* 168: 93–110
- Zeng DD, Qin R, Alamin M, Liang R, Yang CC, Jin XL, Shi CH (2016) *DBOP* specifies palea development by suppressing the expansion of the margin of palea in rice. *Genes Genomics* 38: 1095–1103
- Zhang J, Cai Y, Yan H, Jin J, You X, Wang L, Kong F, Zheng M, Wang G, Jiang L, et al. (2018) A Critical Role of *OsMADS1* in the development of the body of the palea in rice. *J Plant Biol* 61: 11–24
- Zhang T, Li Y, Ma L, Sang X, Ling Y, Wang Y, Yu P, Zhuang H, Huang J, Wang N, et al. (2017) *LATERAL FLORET 1* induced the three-florets spikelet in rice. *Proc Natl Acad Sci USA* 114: 9984–9989
- Zhu QH, Ramm K, Shivakkumar R, Dennis ES, Upadhyaya NM (2004) The *ANTHER INDEHISCENCE1* gene encoding a single MYB Domain protein is involved in anther development in rice. *Plant Physiol* 135: 1514–1525
- Zhu X, Liang W, Cui X, Chen M, Yin C, Luo Z, Zhang D (2015) Brassinosteroids promote development of rice pollen grains and seeds by triggering expression of Carbon Starved Anther, a MYB domain protein. *Plant J* 82: 570–581